VOL. 10, NO 20, NOVEMBER, 2015 ISSN 1819-6608
ARPN Journal of Engineering and Applied Sciences

www.arpnjournals.com

INTERPRETATION OF PRESSURE TESTS IN UNIFORM-FLUX FRACTURED VERTICAL WELLS WITH THRESHOLD PRESSURE GRADIENT IN LOW PERMEABILITY RESERVOIRS

Freddy Humberto Escobar[1], Yu Long Zhao[2], and Maysam Pournik[3], Qi Guo Liu[2] and Guiber Olaya-Marin[1]
[1]Universidad Surcolombiana/CENIGAA, Avenida Pastrana - Cra, Neiva, Huila, Colombia
[2]State Key Laboratory of Oil and Gas Reservoir Geology and Exploitation, Southwest Petroleum University, Xindu Street, xindu district, Chendu, Sichuan, P.R. China
[3]The University of Oklahoma, 100 E. Boyd St. SEC Rm., Norman, OK, USA
E-Mail: fescobar@usco.edu.co

ABSTRACT

The level of pressure gradient needed to enable fluid to overcome the viscous forces and start flowing is referred to as the threshold pressure gradient, TPG, or minimum pressure gradient required for fluid flow. While it has been observed that TPG has an important effect on the pseudorradial flow regime of a fractured vertical well, the early linear flow regime caused by the fracture is not impacted by TPG. In this work, *TDS* methodology is implemented for interpretation of pressure tests in uniform-flux fractured vertical wells of low permeability reservoirs affected by TPG. Two governing equations of the TPG effect on pressure response were developed, in addition to two correlations, which were all tested and validated in a synthetic case.

Keywords: *TDS* technique, pressure transient analysis, vertical fractured wells, flow regimes.

1. INTRODUCTION

An additional pressure gradient is required in low permeability reservoir for the fluid to flow. The onset pressure gradient value for this to happen is known as the threshold pressure gradient. As expressed by the title, the TPG is important in low permeability reservoirs, let us say permeabilities lower than 10 or 20 md.

Raymond and Philip (1963) observed the effect of TPG in flow of water through soils with high clay content. The impact of TPG on the fluid flow through porous materials and its role on the pressure and flow rate distributions were study by Pascal (1981). Yun, Yu, and Cai (2008) introduced a fractal model to capture the Bingham fluids flow in porous media under TPG conditions. The impact of the onset pressure gradient required to initiate fluid flow has been studied by several researchers. Prada and Civan (1999) formulated some empirical correlations for the determination of the minimum pressure gradient as a function of fluid mobility. Their study was based on a laboratory investigation on the effect of the onset pressure gradient on several low permeability rocks.

Lu and Ghedan (2011) presented an analytical solution and conventional analysis of the pressure behavior of vertical wells in low permeability reservoirs under the influence of TPG. Lu (2012) included the effect of TPG on pressure tests in uniform-flux hydraulically fractured vertical wells. These two researches did not consider the effect of wellbore storage coefficient on the pseudorradial flow regime when TPG effects are included. As seen later in the present study, these effects are quite important.

Owayed and Tiab (2008) presented an analytical solution and interpretation technique of the flow of a slightly compressible Bingham fluid. Zhao *et al*. (2013) presented an analytical solution for the horizontal well transient pressure behavior of a naturally-fractured reservoir with the effect of TPG. They observed that the impact of TPG is only observed during pseudorradial flow regime. Escobar *et al*. (2014b) used the model presented by Zhao *et al.* (2013) to formulate an interpretation methodology based upon *TDS* technique, Tiab (1993).

The studies of Zhao *et al.* (2013) and Escobar *et al*. (2013) show the effect of the threshold pressure gradient is easily observed by an upwards deviation of the pressure derivative during pseudorradial flow regime. A similar situation is observed in the present work where the impact is also seen on the pseudorradial flow regime. This situation is expected to take place since the pseudorradial flow in a horizontal well is the same as the radial flow in a vertical well.

It is also necessary to clarify that all the former studies, even the present one, assume a porous medium filled with a Newtonian-type fluid. As seen in the recent works by Escobar, Martinez and Montealegre (2010) and Escobar et al. (2011) the pressure derivative during radial flow regime is affected by the flow behavior index, *n*, then this effect is excluded from the present work.

It was also observed that as the wellbore storage coefficient increases so does the slope of the pressure derivative curve during radial/pseudorradial flow regime. Since fractured wells are normally tested under bottom-hole shut-in conditions; then, wellbore storage was assumed to be negligible in the present study.

The main objective of this work is to introduce an interpretation technique based upon observations from the pressure and pressure derivative plot for developing analytic expressions and correlations to estimate the dimensionless threshold pressure gradient. Two defined tendencies were identified due to the influence of the TPG; then, governing equations for these were developed. The new expressions were successfully tested with a synthetic example.

2. MATHEMATICAL FORMULATION

2.1. Modeling

The uniform-flux fractured vertical well model used in this work is an integration of the point-source function along the fracture, which is derived in the work presented by Zhao *et al.* (2013).

2.2. Dimensionless quantities

The dimensionless quantities considered in this study are given below.

$$t_{D_{xf}} = \frac{0.0002637kt}{\phi\mu c_t x_f^2} \quad (1)$$

$$P_D = \frac{kh\Delta P}{141.2q\mu B} \quad (2)$$

$$t_D * P_D' = \frac{kh(t*\Delta P')}{141.2q\mu B} \quad (3)$$

$$t_D^2 * P_D'' = \frac{kh(t^2*\Delta P'')}{141.2q\mu B} \quad (4)$$

$$PG_D = \frac{k_h r_w h(PG)}{141.2q\mu B} \quad (5)$$

$$C_D = \frac{0.894C}{\phi c_t h x_f^2} \quad (6)$$

2.2. Pressure, pressure derivative and second pressure derivative behaviors

Different pressure scenarios were obtained using the model adapted from the work of Zhao *et al.* (2012). Pressure and pressure derivative behavior for different dimensionless pressure gradient values (which represents different TPG values) expected to occur in field situations are shown in Figure-1. It is important to note that the early pressure data during the fracture-acting time period remain unaltered, as flow is dominated by fracture flow and there is no impact of TPG on flow in high permeability fracture However, pressure derivative during pseudorradial flow regime deviates upwards from the horizontal line (with TPG = 0) making it difficult to obtain permeability due to TPG masking the pseudorradial flow regime. As dimensionless pressure gradient increases from 0 to 0.1, there is greater deviation and masking of pseudorradial flow regime with more inclined line from horizontal. It is interesting to notice that at late pseudorradial flow regime time, both pressure and pressure derivative are present and half-slope line behavior similar to the linear flow regime is observed.

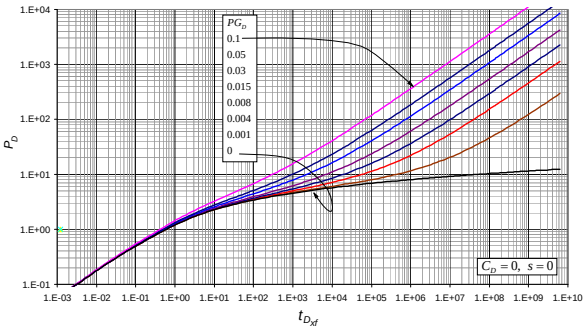

Figure-1. Dimensionless pressure vs. time for different dimensionless pressure gradient values of a vertical fractured well in an infinite homogeneous reservoir.

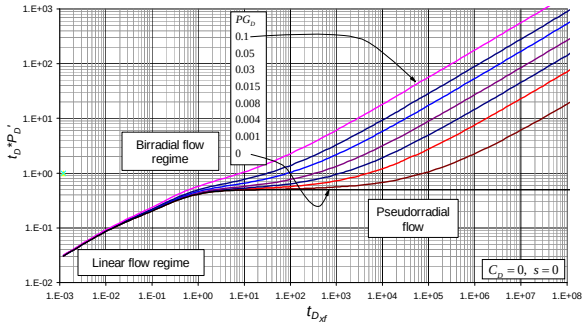

Figure-2. Dimensionless pressure derivative vs. time for different dimensionless pressure gradient values of a vertical fractured well in an infinite homogeneous reservoir.

In order to observe more features of the effect of TPG, log-log plot of second (numerical) pressure derivative versus time is drawn in Figure-3. There is a clear minima and maxima observed on the plot with the half-slope behavior as well.

Effect of wellbore storage on pressure response for a given dimensionless pressure gradient is shown in Figure-4. Clearly, wellbore storage impacts the pressure and pressure derivative behavior by shifting upward the

pressure derivative as dimensionless wellbore storage increases. In this study, the focus is on investigating and predicting effect of TPG in pressure response, hence wellbore storage is assumed to be zero. The combined effect of wellbore storage and TPG will be investigated in future work.

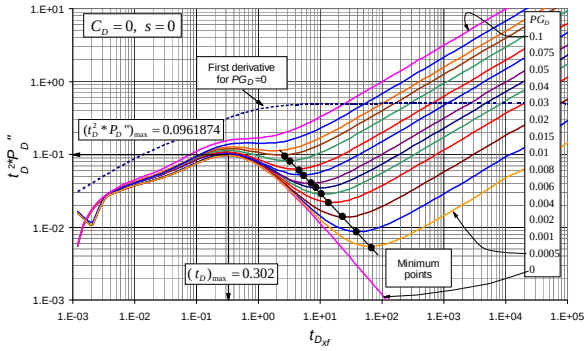

Figure-3. Dimensionless second pressure derivative vs. time for different dimensionless pressure gradient values of a vertical fractured well in an infinite homogeneous reservoir.

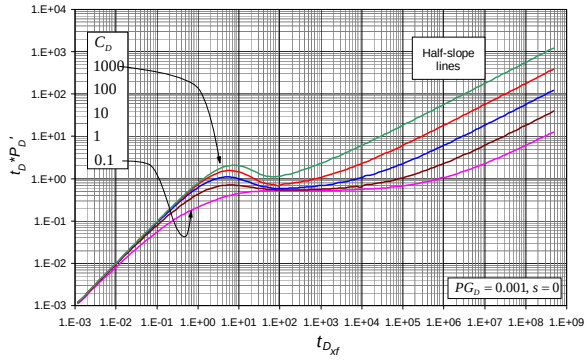

Figure-4. Effect of wellbore storage on the dimensionless pressure derivative vs. time for a constant dimensionless pressure gradient and skin factor.

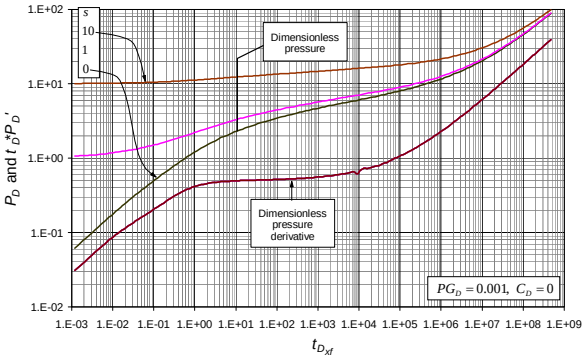

Figure-5. Effect skin factor on the dimensionless pressure and pressure derivative vs. time for a constant dimensionless pressure gradient and zero wellbore storage coefficient.

Figure-5 shows the effect of skin factor on pressure response under a fixed value of dimensionless pressure gradient. As expected, skin factor affects the dimensionless pressure but does not affect the pressure derivative since in the model the skin factor is time independent then its derivative will be zero. Fractured wells are expected to have small skin factor values (less than 10), which show no significant effect on the pressure derivative behavior.

2.3. *TDS* technique

The main objective of this paper is to provide a practical methodology following the *TDS* technique philosophy, Tiab (1993), for interpretation of well pressure data under the effect of threshold pressure gradient. Tiab (1993) demonstrated that permeability and skin factor can be obtained from data obtained during pseudorradial flow regime;

$$k = \frac{70.6 q \mu B}{h(t * \Delta P')_r} \tag{7}$$

$$s = 0.5\left(\frac{\Delta P_r}{(t * \Delta P')_r} - \ln\left[\frac{k\, t_r}{\phi \mu c_t r_w^2}\right] + 7.43\right) \tag{8}$$

The above equations assume that the pseudorradial flow regime is easily identified with a horizontal line formed by the pressure derivative during pseudorradial flow regime, $(t*\Delta P')_r$, which is not the case for wells affected by TPG (see Figure-2). The solution of this study need to know the value of the pressure derivative during pseudorradial flow regime, $(t*\Delta P')_r$, meaning permeability has to be known from either a former pressure test or from other source. In any case, the pseudorradial flow regime pressure derivative can be solved from Equation (7):

$$(t*\Delta P')_r = \frac{70.6q\mu B}{hk} \quad (9)$$

If the typical horizontal line of the pressure derivative during pseudorradial flow is not observed in the test and permeability is also unknown, pressure derivative is then used to find reservoir permeability. As seen in Figure-3, once linear flow regime vanishes, the second pressure derivative will always displays a maximum point which has coordinates for zero dimensionless pressure gradient of:

$$(t_D^2 * P_D'')_{\max} = 0.0961874 \quad (10)$$

$$(t_{Dxf})_{\max} = 0.302 \quad (11)$$

If checking back again in the maximum point of Figure-3, notice that the second pressure derivative maximum is affected by the dimensionless pressure gradient but the maximum time remains unaltered. Then, after plugging the dimensionless time quantity given by Equation (1), permeability can be estimated if the half-fracture length is known.

$$k = \frac{1145.24\phi\mu c_t x_f^2}{t_{\max}} \quad (12)$$

However, if the half-fracture length is unknown, one can use the maximum point of the second pressure derivative to find a correlation for permeability determination. Notice also that the maximum point is affected by the pressure gradient in a perfect linear proportion as indicated by Figure-6. Based on this observation, a correction for expression (9) is given by Equation (12) as:

$$(t_D^2 * P_D'')_{\max} = 0.0962\left[9.2119\frac{(t_D^2 * P_D'')_{\max}}{(t_D * P_D')_{L1}}\right]^{-1} \quad (13)$$

Once the dimensionless quantities given by Equations (3) and (4) are replaced in Equation (13) an expression for estimating the formation permeability is obtained:

$$k = \frac{1.475q\mu B(t*\Delta P')_{L1}}{h(t^2*\Delta P'')^2_{\max}} \quad (14)$$

Notice that Equation (12) uses also the reading of the pressure derivative during linear flow regime at a time of 1 hr, $(t*\Delta P')_{L1}$, extrapolated if needed.

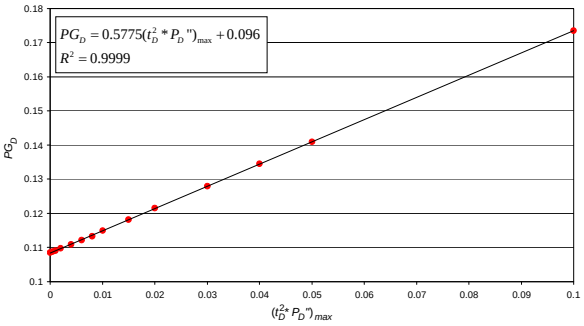

Figure-6. Relationship between the dimensionless pressure gradient and the maximum dimensionless second pressure derivative.

Once permeability is known, the next step is to determine the dimensionless pressure gradient. For that purpose, the effect of this parameter is unified by multiplying the dimensionless time by the square of the dimensionless pressure gradient, with behavior shown in Figure-7. Two important features are seen during pseudorradial flow regime: (1) a quarter-slope (*qs*) straight line and (2) half-slope (*hs*) straight line which governing equations are, respectively, given by:

$$(t_D * P_D)_{qs} = \sqrt[4]{\frac{36}{10}PG_D^2\pi(t_{Dxf})_{qs}} \quad (15)$$

$$(t_D * P_D')_{hs} = \sqrt{PG_D^2\pi(t_{Dxf})_{hs}} \quad (16)$$

Solving for the dimensionless pressure gradient from the above equations leads to:

$$PG_D = \frac{x_f}{1088.8}\left(\frac{h(t*\Delta P')_{qs}}{qB}\right)^2\sqrt{\frac{k^3\phi c_t}{\mu^3 t_{qs}}} \quad (17)$$

$$PG_D = \frac{h(t*\Delta P')_{hs}x_f}{4.064qB}\sqrt{\frac{k\phi c_t}{\mu t_{hs}}} \quad (18)$$

The above expressions use a value of the pressure derivative read at any arbitrary time during the given behavior. However, for best interpretation, it is recommended to read these values at a time of 1 hr so Equations (17) and (18) become:

$$PG_D = \frac{x_f}{1088.8}\left(\frac{h(t*\Delta P')_{qs1}}{qB}\right)^2\sqrt{\frac{k^3\phi c_t}{\mu^3}} \quad (19)$$

$$PG_D = \frac{h(t*\Delta P')_{hs1} x_f}{4.064qB}\sqrt{\frac{k\phi c_t}{\mu}} \quad (20)$$

If both half slope and quarter slope lines are observed, the dimensionless pressure gradient can be also found from intersection point of these two lines, $t_{qs\_hs\_i}$, so:

$$PG_D = 57.53 x_f \sqrt{\frac{\phi\mu c_t}{k t_{qs\_hs\_i}}} \quad (21)$$

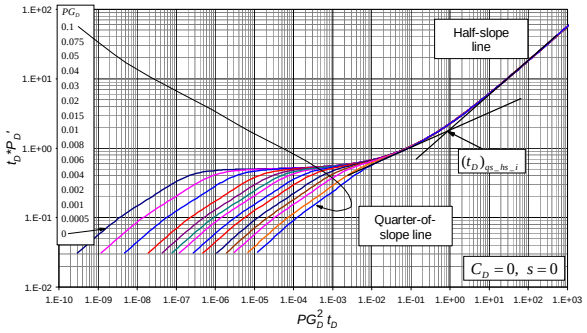

Figure-7. Dimensionless pressure derivative vs. the product of dimensionless pressure gradient in second power with the dimensionless time.

In case that neither line is observed due to either a short test or noise, then two key parameters of the second pressure derivative are used for the estimation of the pressure gradient: (a) the maximum point, and (b) the minimum points. Figure-8 expresses the existing relationship between the maximum second pressure derivative and pseudorradial pressure derivative value with the dimensionless pressure gradient. The following correlation is obtained:

$$PG_D = 0.8658[(t_D^2 * P_D'')_{\max} / (t_D * P_D')_r] - 0.1663 \quad (22)$$

After replacing Equations (3) and (4) in the above expression leads to:

$$PG_D = 0.8658[(t^2 * \Delta P'')_{\max} / (t * \Delta P')_r] - 0.1663 \quad (23)$$

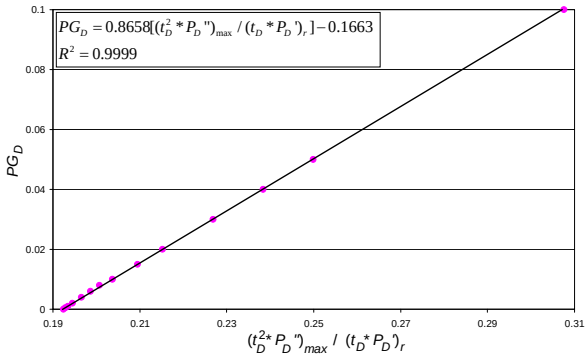

Figure-8. Relationship between the ratio of the maximum second pressure derivative at the maximum point and the pressure derivative during pseudorradial flow regime with the dimensionless pressure gradient.

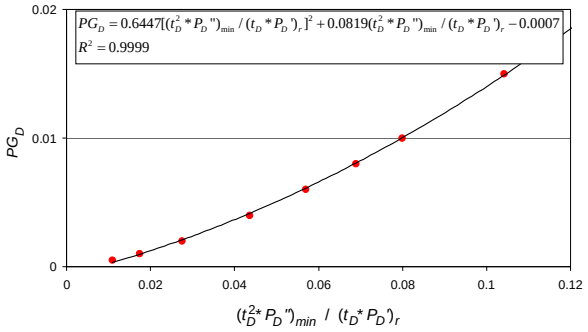

Figure-9. Relation between the minimum second pressure derivative and the dimensionless pressure gradient.

The relationship between the minimum second pressure derivatives is given in Figure-9 from which the following correlation is derived:

$$PG_D = 0.6447[(t_D^2 * P_D'')_{\min} / (t_D * P_D')_r]^2 + 0.0819(t_D^2 * P_D'')_{\min} / (t_D * P_D')_r - 0.0007 \quad (24)$$

Also, after replacing Equations (3) and (4) in the above expression leads to:

$$PG_D = 0.6447[(t^2 * \Delta P'')_{\min} / (t * \Delta P')_r]^2 + 0.0819(t^2 * \Delta P'')_{\min} / (t * \Delta P')_r - 0.0007 \quad (25)$$

Finally, the half- fracture length determination by the *TDS* technique was presented by Tiab (1994):

$$x_f = \frac{2.032qB}{h(t*\Delta P')_{L1}}\sqrt{\frac{\mu}{\xi\phi c_t k}} \quad (26)$$

Where $(t^*\Delta P')_{L1}$ is the pressure derivative during the early time linear flow regime read a time of 1 hr, extrapolated if necessary. Notice that ξ was original excluded in Tiab's model since it was only presented for homogeneous formations. ξ was introduced by Escobar *et al*. (2014a). Then, when $\xi = 1$, Equation (26) accounts for homogeneous reservoirs. For the case of naturally-fractured formations, $\xi = \omega$ which is the dimensionless storativity coefficient.

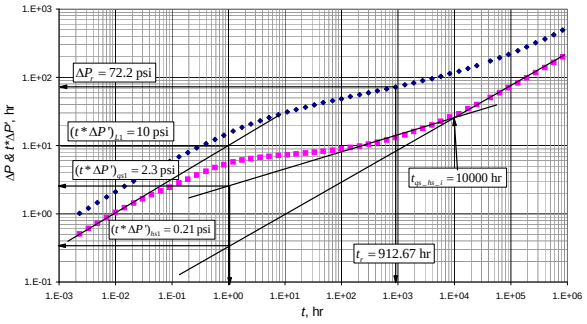

Figure-10. Pressure and pressure derivative versus time for example.

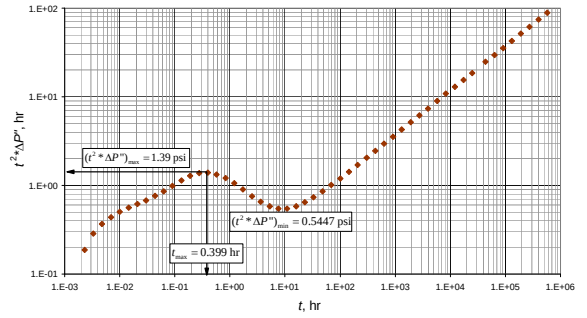

Figure-11. Second pressure derivative versus time for example.

3. DETAILED SYNTHETIC EXAMPLE

Pressure data is given in Table-1. Also, the pressure drop and pressure derivative versus time log-log plot for a simulated drawdown is provided in Figure-10 and the second pressure derivative versus time log-log plot for the same exercise is given in Figure-11. The input data for the simulation is given as follows:

q = 35 BPD	B = 1.2 rb/STB
μ = 2.3 cp	c_t = 1x10^{-5} psi^{-1}
h = 100 ft	k = 10 md
ϕ = 5 %	x_f = 55 md
PG_D = 0.01	s = 0

Solution: The following information was read from Figures-10 and 11,

ΔP_r = 72.2 psi	$(t^*\Delta P')_{L1}$ = 12 psi
$(t^*\Delta P')_{qs1}$ = 2.3 psi	$(t^*\Delta P')_{hs1}$ =0.21 psi
$t_{qs\_hs\_i}$ =10000 hr	t_{max} =0.399 hr
$(t^2*\Delta P")_{max}$ = 1.38 psi	$(t^2*\Delta P")_{min}$ = 0.5447 psi
t_r = 912.67 hr	

The procedure is outlined as follows:

Step-1: Determine reservoir permeability using Equation (14):

$$k = \frac{1.475(35)(2.3)(1.2)(11)}{100(1.38)^2} = 8.23 \text{ md}$$

Step-2: Find half-fracture length with Equation (26):

$$x_f = \frac{2.032(35)(1.2)}{100(11)}\sqrt{\frac{2.3}{(1)(0.05)(1\times10^{-5})(8.23)}} = 58 \text{ ft}$$

Step-3: Recalculate permeability with Equation (12):

$$k = \frac{1145.24(0.05)(2.3)(1\times10^{-5})58^2}{0.399} = 11.1 \text{ md}$$

Step-4: Since the two permeability values are around the target of 10 md, it is good to obtain the arithmetic average which is 9.67 md.

Step-5: Find the pseudorradial pressure derivative corresponding to the permeability value found in step 4.

$$(t^*\Delta P')_r = \frac{70.6(35)(2.3)(1.2)}{(100)(9.67)} = 7.06 \text{ psi}$$

Step-6: Find the dimensionless pressure gradient with Equations (19), (20) and (21) (all from observed pressure response);

$$PG_D = \frac{58}{1088.8}\left(\frac{100(2.3)}{(35)(1.2)}\right)^2\sqrt{\frac{9.67^3(0.05)(1\times10^{-5})}{2.3^3}} = 0.0098$$

$$PG_D = \frac{100(0.21)(58)}{4.064(35)(1.2)}\sqrt{\frac{9.67(0.05)(1\times10^{-5})}{2.3}} = 0.0103$$

$$PG_D = 57.53(58)\sqrt{\frac{(0.05)(2.3)(1\times10^{-5})}{9.67(10000)}} = 0.0109$$

Table-1. Pressure drop, pressure derivative and second pressure derivative versus time data.

t, hr	ΔP, psi	$t^*\Delta P'$, psi	$t^2*\Delta P''$, psi
0.00229	1.010	0.506	0.187
0.00331	1.215	0.609	0.286
0.00479	1.462	0.732	0.367
0.00692	1.758	0.876	0.439
0.01001	2.112	1.043	0.505
0.01446	2.530	1.229	0.562
0.02091	3.020	1.432	0.617
0.03022	3.588	1.654	0.679
0.04368	4.240	1.896	0.758
0.06314	4.985	2.165	0.862
0.09127	5.835	2.471	0.993
0.13192	6.808	2.825	1.140
0.1907	7.923	3.238	1.277
0.2756	9.204	3.710	1.369
0.3984	10.671	4.228	1.389
0.5759	12.332	4.762	1.331
0.8324	14.186	5.277	1.210
1.2031	16.215	5.742	1.055
1.7391	18.399	6.140	0.897
2.5137	20.713	6.468	0.758
3.6334	23.136	6.736	0.651
5.25	25.650	6.961	0.581
7.59	28.244	7.158	0.548
10.97	30.911	7.344	0.549
15.86	33.649	7.532	0.581
22.93	36.461	7.735	0.643
33.14	39.353	7.962	0.733
47.90	42.337	8.225	0.854
69.23	45.425	8.533	1.007
100.07	48.636	8.897	1.197
144.65	51.994	9.330	1.429
209.08	55.527	9.848	1.711
302.21	59.268	10.469	2.053
436.83	63.259	11.212	2.465
631.41	67.550	12.105	2.961
912.67	72.203	13.177	3.558
1319.21	77.288	14.465	4.276
1906.83	82.895	16.014	5.140
2756.21	89.127	17.874	6.180
3983.94	96.113	20.111	7.315
5758.55	104.003	22.800	8.997
8323.64	112.981	26.032	10.839
12031.31	122.997	29.169	12.947
17390.54	135.279	34.910	15.430
25136.98	148.874	40.207	18.536
43683.06	173.842	50.597	24.687
63141.24	194.162	59.499	29.636
91266.86	218.141	70.437	35.547
131920.74	246.365	83.262	42.750
190683.49	279.854	98.773	51.376
275621.50	319.573	117.374	61.779
398394.28	366.817	139.734	74.283
575854.93	423.104	166.610	89.309
832363.62	490.281	198.941	107.381

All the above equations give very close values to the actual dimensionless pressure gradient, which shows the validity of all of the above equations.

Step-7: Use correlation given by Equation (23) to estimate the dimensionless pressure gradient. The ratio of the maximum second pressure derivative and the pseudorradial pressure derivative is 0.197, then:

$$PG_D = 0.8658[0.197] - 0.1663 = 0.0042$$

This value does not respond well to the actual value as it is based on a correlation.

Step-8: Use correlation given by Equation (25) to estimate the dimensionless pressure gradient. The ratio of the minimum second pressure derivative and the pseudorradial pressure derivative is 0.0772, then:

$$PG_D = 0.6447[0.0772]^2 + 0.0819(0.0772) - 0.0007 = 0.0095$$

4. COMMENTS ON THE RESULTS

The agreement between the simulated and estimated results in the worked example show that the equations and corrections introduced in this study work very well with a slight exception of Equation (23) which is a correlation. However, four accepted values of the dimensionless pressure gradient were estimated from the simulated test.

5. CONCLUSIONS

a) Extension of the *TDS* technique was given for the case of vertical wells with pressure gradient threshold. Two governing equations for the influence of this parameter during pseudorradial flow regime were developed and successfully tested by a simulated example.
b) The higher the TPG the more deviated upwards the pressure derivative pseudorradial flow regime from its characteristic horizontal behavior. It was also found that the wellbore storage coefficient has a combined impact with the TPG during pseudorradial flow regime. Then, an analytical solution for unfractured wells should be developed.
c) This work also includes the estimation of the formation permeability in spite of the absence of the horizontal behavior of the pressure derivative during pseudorradial flow regime. In this work, both the maximum point of the pressure derivative once linear flow vanishes and the reading of the fracture linear behavior read at a time of 1 hr is used for predicting reservoir permeability.

ACKNOWLEDGEMENTS

The work financially supported by 973 Program of China under Grant No. 2014CB239205 and the Natural Science Foundation of China (Grant No. 51374181). The authors gratefully thank Universidad Surcolombiana, the University of Oklahoma and the State Key Laboratory of Oil and Gas Reservoir Geology and Exploitation in Southwest Petroleum University.

Nomenclature

B	Volumetric factor, rb/Mscf
c_t	System total compressibility, 1/psi
k	Permeability, md
h	Reservoir thickness, ft
P	Pressure, psi
PG	Threshold pressure gradient, psi/ft
PG_D	Dimensionless threshold pressure gradient
r	Radius, ft
s	Skin factor
t	Time, hr
t_D	Dimensionless time
$t*\Delta P'$	Pressure derivative, psi
$t^2*\Delta P''$	Second pressure derivative, psi
t_D*P_D'	Dimensionless pressure derivative
$t_D^2*P_D''$	Dimensionless second pressure derivative, psi
x_f	Half-fracture length, ft

Greeks

ϕ	Porosity, fraction
μ	Viscosity, cp

Suffices

D	Dimensionless
Dxf	Dimensionless based on half-fracture length
ELL	Elliptical
f	Fracture
hs	Half slope
hs	Half slope read at 1 hr
L	Linear
*L*1	Linear at 1 hr
max	Maximum
min	Minimum
qs	Quarter slope
*qs*1	Quarter slope read at 1 hr
qs_hs_i	Intercept between quarter slope and half slope lines

REFERENCES

Escobar F.H., Martínez J.A. and Montealegre-M. M. 2010. Pressure and Pressure Derivative Analysis for a Well in a Radial Composite Reservoir with a Non-Newtonian/Newtonian Interface. CT and F. 4(1): 33-42.

Escobar F.H., Zambrano A.P, Giraldo D.V. and Cantillo J.H. 2011. Pressure and Pressure Derivative Analysis for Non-Newtonian Pseudoplastic Fluids in Double-Porosity Formations. CT and F. 5(3): 47-59.

Escobar F.H., Ghisays-Ruiz A. and Bonilla L.F. 2014a. New Model for Elliptical Flow Regime in Hydraulically-Fractured Vertical Wells in Homogeneous and Naturally-Fractured Systems. Journal of Engineering and Applied Sciences. 9(9): 1629-1636.

Escobar F.H., Zhao Y.L. and Zhang L.H. 2014b. Interpretation of Pressure Tests in Horizontal Wells in Homogeneous and Heterogeneous Reservoirs with Threshold Pressure Gradient. Journal of Engineering and Applied Sciences. 9(11): 2220-2228.

Lu J. and Ghedan S. 2011. Pressure behavior of vertical wells in low-permeability reservoirs with threshold

pressure gradient. Special Topics and Reviews in Porous Media. 2(3): 157-169.

Lu J. 2012. Pressure behavior of uniform-flux hydraulically fractured wells in low-permeability reservoirs with threshold pressure gradient. Special Topics and Reviews in Porous Media-An International Journal. 3(4): 307-320.

Owayed J.F. and Tiab D. 2008. Transient pressure behavior of Bingham non-Newtonian fluids for horizontal wells Journal of Petroleum Science and Engineering. 61: 21-32.

Pascal H. 1981. Nonsteady flow through porous media in the presence of a threshold gradient. Acta Mechanica 39 207-224.

Prada A. and Civan F. 1999. Modification of Darcy's law for the threshold pressure Gradient. Journal of Petroleum Science and Engineering. 22: 237-240.

Raymond J. M. and Philip F. L. 1963. Threshold Gradient for water flow in clay systems Soil Science Society of America Journal. 27: 605-609.

Tiab D. 1993. Analysis of Pressure and Pressure Derivative without Type-Curve Matching: 1- Skin and Wellbore Storage. Journal of Petroleum Science and Engineering. 12: 171-181.

Tiab D. 1994. Analysis of Pressure Derivative without Type-Curve Matching: Vertically Fractured Wells in Closed Systems. Journal of Petroleum Science and Engineering. 11: 323-333.

Yun M. J., Yu B.M. and Cai J.C. 2008. A fractal model for the starting pressure gradient for Bingham fluids in porous media International Journal of Heat and Mass Transfer. 51: 1402-1408

Zhao Y.L., Zhang L.H., Feng W., Zhang B.N and Lis Q.G. 2013. Analysis of horizontal well pressure behavior in fractured low permeability reservoirs with consideration of the threshold pressure gradient. Journal of Geophysics and Engineering. 10: 1-10.